

Probing neutrino mass hierarchies and ϕ_{13} with supernova neutrinos

Shao-Hsuan Chiu*

Physics Group, C.G.E., Chang Gung University, Kwei-Shan 333, Taiwan

T. K. Kuo†

Department of Physics, Purdue University, West Lafayette, IN 47907

Abstract

We investigate the feasibility of probing the neutrino mass hierarchy and the mixing angle ϕ_{13} with the neutrino burst from a future supernova. An inverse power-law density $\rho \sim r^n$ with varying n is adopted in the analysis as the density profile of a typical core-collapse supernova. The survival probabilities of ν_e and $\bar{\nu}_e$ are shown to reduce to two-dimensional functions of n and ϕ_{13} . It is found that in the $n - \sin^2 \phi_{13}$ parameter space, the 3D plots of the probability functions exhibit highly non-trivial structures that are sensitive to the mass hierarchy, the mixing angle ϕ_{13} , and the value of n . The conditions that lead to observable differences in the 3D plots are established. With the uncertainty of n considered, a qualitative analysis of the Earth matter effect is also included.

Typeset using REVTeX

*schiu@mail.cgu.edu.tw

†tkkuo@physics.purdue.edu

I. INTRODUCTION

A better knowledge of the neutrino property is regarded as one of the crucial keys in searching for new physics beyond the standard model. Recent experiments of neutrino oscillation have been able to uncover part of the neutrino properties, such as the neutrino mixing angles and the mass squared differences responsible for the solar neutrino problem and the atmospheric neutrino deficit [1–5]. However, there exists an ambiguity in the sign of the squared difference $\Delta m_{32}^2 \equiv m_3^2 - m_2^2$ involved in the oscillation of atmospheric neutrinos. The two scenarios are referred to as the normal ($m_3 \gg m_2, m_1$) and the inverted ($m_2, m_1 \gg m_3$) mass hierarchies. Furthermore, although an upper bound on the mixing angle ϕ_{13} is established by $\sin^2 \phi_{13} < 0.02$ [6,7], a definite determination of this angle has not been achieved yet.

The rich physical content of a core-collapse supernova makes the supernova neutrino one of the most promising tools for the study of unknown neutrino properties and the supernova mechanism [8]. The supernova neutrinos are unique in that both neutrinos and antineutrinos are produced at very high densities and high temperatures before propagating through matter of varying densities. Due to the wide range of matter density in a supernova, the neutrinos may go through two or even three (if the regeneration effect due to the Earth matter occurs) separate flavor conversions before reaching the terrestrial detectors. Furthermore, the matter-enhanced oscillations [9,10] in a core-collapse supernova lead to a striking feature that a small variation of the mixing angle ϕ_{13} can significantly alter the neutrino spectra. For supernova neutrinos, the main physical consequence arising from the ambiguity of the mass hierarchy is that both the higher and the lower level crossings occur in the ν sector if the mass hierarchy is normal, while the higher crossing occurs in the $\bar{\nu}$ sector and the lower crossing occurs in the ν sector if the mass hierarchy is inverted.

The future galactic supernova is capable of inducing roughly 10^4 neutrino events at the terrestrial detectors, and is expected to provide a much better statistics than the SN1987A [11] did. This promising characteristic has motivated a wealth of discussions on how the neutrino fluxes from a supernova can facilitate the search of the unknown neutrino properties [12–18]. As generally realized, the main difficulty in extracting information from the supernova neutrinos arises from the poorly known exploding mechanism. Incomplete knowledge of the supernova leads to, among others, an uncertainty in the density profile of a supernova.

The supernova neutrinos are usually assumed to propagate outward through an inverse power-law matter density, $\rho \sim r^n$, with $n = -3$. However, due to lack of statistically significant real data, there is no clear evidence showing that the density distribution $\rho \sim r^{-3}$ provides a reliable connection between the dynamics of flavor conversion and the expected neutrino events at the detectors. In addition, the shock propagation in a supernova [19] represents a time-dependent disturbance to the matter density and causes a sizable effect to the neutrino flavor conversion. Since only the matter density near a resonance point is relevant to the flavor conversion and any local deviation from $n = -3$ cannot be ruled out, the profile $\rho \sim r^{-3}$ should not be considered as a satisfactory description to the density shape for the purpose of extracting neutrino properties from the observation of supernova neutrinos.

In this work, possible consequences resulting from variation of the density profile are

examined. The aim is to analyze the neutrino survival probabilities and to study how the uncertainty in n would affect the determination of the mixing angle ϕ_{13} and the mass hierarchy. This paper is organized as follows. In Section II, we outline the n -dependent formulation of the survival probabilities for ν_e and $\bar{\nu}_e$. In section III, parameters obtained from the solar, the atmospheric, and the terrestrial experiments are taken as the input for constructing the 3D plots of the probability functions. The probability functions under both the normal and the inverted mass hierarchies are analyzed. In section IV, we discuss the feasibility of probing the neutrino mass hierarchy and ϕ_{13} with the properties of the probability functions. In section V, the discussion is expanded to include the Earth matter effect. We then summarize this work in section VI.

II. CONVERSION PROBABILITIES

The density profile of matter encountered by the propagating neutrinos plays a crucial role in the dynamics of flavor conversion. In the literature, the neutrino flavor conversion in media of various density profiles has been widely discussed. However, the exact solution is obtained only for a few specific density distributions : the linear, exponential, hyperbolic tangent, and the $1/r$ profiles. It was suggested [20] that for an arbitrary inverse power-law density $\rho \sim r^n$, an extra correction factor F (a function of n and the mixing angle) can be supplemented to the standard Landau-Zener [21] formulation of the level crossing to account for the effect due to deviation from a linear density profile.

With the extremely high electron number density in a supernova, the effective mixing angles in matter for the neutrino and the antineutrino become $\phi_{13}^m \approx \pi/2$, $\theta_{12}^m \approx \pi/2$ and $\bar{\phi}_{13}^m \approx 0$, $\bar{\theta}_{12}^m \approx 0$, respectively. Using the standard parametrization of the neutrino mixing matrix: $U_{e1}^2 = \cos^2 \phi_{13} \cos^2 \theta_{12}$, $U_{e2}^2 = \cos^2 \phi_{13} \sin^2 \theta_{12}$, and $U_{e3}^2 = \sin^2 \phi_{13}$, the survival probabilities for ν_e and $\bar{\nu}_e$ can be written respectively as [22,13]

$$P_{nor} = U_{e1}^2 P_l P_h + U_{e2}^2 (1 - P_l) P_h + U_{e3}^2 (1 - P_h), \quad (1)$$

$$\bar{P}_{nor} = U_{e1}^2 (1 - \bar{P}_l) + U_{e2}^2 \bar{P}_l, \quad (2)$$

for the normal hierarchy and

$$P_{inv} = U_{e2}^2 (1 - P_l) + U_{e1}^2 P_l, \quad (3)$$

$$\bar{P}_{inv} = U_{e2}^2 \bar{P}_l \bar{P}_h + U_{e1}^2 (1 - \bar{P}_l) \bar{P}_h + U_{e3}^2 (1 - \bar{P}_h), \quad (4)$$

for the inverted hierarchy. Note that P_h (\bar{P}_h) and P_l (\bar{P}_l) represent the higher and the lower level crossing probabilities for ν_e ($\bar{\nu}_e$), respectively. For arbitrary density profile and mixing angle, the Landau-Zener formula is modified as

$$P_{h,l} = \frac{\exp(-\frac{\pi}{2} \gamma_{h,l} F_{h,l}) - \exp(-\frac{\pi}{2} \gamma_{h,l} \frac{F_{h,l}}{\sin^2 \Theta_{ij}})}{1 - \exp(-\frac{\pi}{2} \gamma_{h,l} \frac{F_{h,l}}{\sin^2 \Theta_{ij}})}, \quad (5)$$

where $\gamma_{h,l}$ are the adiabaticity parameters, Θ_{ij} are the mixing angles between the i th and the j th mass eigenstates, and $F_{h,l}$ are the correction factors to a non-linear profile. Note that $P_h = \bar{P}_h$, and that \bar{P}_l can be obtained directly from P_l by replacing Θ_{ij} with $\pi/2 - \Theta_{ij}$.

For a typical core-collapse supernova, the electron number density can be written as $N_e = (\frac{Y_e}{m_n})cr^n$, where Y_e is the electron number per baryon, m_n is the baryon mass, and c is a constant representing the scale of the density¹. The adiabaticity parameter for this density profile has the general form

$$\gamma_{h,l} = \frac{1}{2|n|} \left(\frac{\Delta m_{ij}^2}{E} \right)^{1+\frac{1}{n}} \left(\frac{\sin^2 2\Theta_{ij}}{\cos 2\Theta_{ij}} \right) \left(\frac{\cos 2\Theta_{ij}}{2\sqrt{2}G_F \frac{Y_e}{m_n} c} \right)^{\frac{1}{n}}, \quad (6)$$

where G_F is the Fermi constant, E is the neutrino energy, and $\Delta m_{ij}^2 \equiv |m_i^2 - m_j^2|$. In the numerical calculation, it would be more convenient to write F_h and F_l as the Euler integral representation of the hypergeometric function:

$$\begin{aligned} F_{h,l} &= {}_2F_1\left(\frac{n-1}{2n}, \frac{2n-1}{2n}; 2; -\tan^2 2\Theta_{ij}\right) \\ &= \frac{\Gamma(2)}{\Gamma(\frac{2n-1}{2n})\Gamma(2-\frac{2n-1}{2n})} \int_0^1 t^{(\frac{2n-1}{2n}-1)} (1-t)^{(2-\frac{2n-1}{2n}-1)} [1-t(-\tan^2 2\Theta_{ij})]^{(\frac{n-1}{2n})} dt. \end{aligned} \quad (7)$$

The above expressions for $P_{h,l}$, $\gamma_{h,l}$, and $F_{h,l}$ can be applied to an arbitrary profile and to both large or small mixing angles. It was pointed out [24,25] that there exists a subtlety in the physical meaning of resonance conversion: For the large mixing angle, the adiabaticity parameters, γ_h and γ_l , should each be calculated at the point of maximum violation of adiabaticity (PMVA) instead of the point of resonance. Note that while the values of $\gamma_{h,l}$ depend on the locations where they are calculated, the values of $\gamma_h F_h$ and $\gamma_l F_l$ remain invariant. To simplify the calculation, we choose to evaluate $\gamma_h F_h$ and $\gamma_l F_l$ at the locations of resonance.

III. NUMERICAL ANALYSIS OF P AND \bar{P}

With the numerical input of Δm_{21}^2 , Δm_{32}^2 , θ_{12} , and c (see, *e.g.*, ref. [14] and the references therein), the survival probability functions $P = P(\Delta m_{21}^2, \Delta m_{32}^2, \phi_{13}, \theta_{12}, E_\nu, n, c)$ and $\bar{P} = \bar{P}(\Delta m_{21}^2, \Delta m_{32}^2, \phi_{13}, \theta_{12}, E_{\bar{\nu}}, n, c)$ reduce to $P = P(E_\nu, n, \phi_{13})$ and $\bar{P} = \bar{P}(E_{\bar{\nu}}, n, \phi_{13})$, respectively. The ambiguity of the mass hierarchy gives rise to four distinct probability functions to be investigated: P_{nor} , \bar{P}_{nor} for the normal hierarchy and P_{inv} , \bar{P}_{inv} for the inverted hierarchy. Their properties can be examined by a series of 3D plots in the $E - \sin^2 \phi_{13}$ parameter space. As an illustration, we show only the 3D plots of P_{nor} for several n values in Fig. 1. From the 3D plots of P_{nor} , \bar{P}_{nor} , P_{inv} , and \bar{P}_{inv} , it can be concluded that all the probabilities exhibit no significant energy dependence except for the low energy end. This behavior implies that when the adiabaticity parameters in Eq. (6) are calculated, the impact coming from the variation of n and ϕ_{13} dominate over that of the variation of energy in the typical range, $E < 10^2$ MeV.

¹The value of c varies very weakly with r over the range $10^{12} g/cm^3 < \rho < 10^{-5} g/cm^3$ [23].

Since the neutrino population is extremely small at the low energy end of the spectrum, it would be convenient to simply take the average energies, *e.g.*, $\langle E_\nu \rangle = 12$ MeV and $\langle E_{\bar{\nu}} \rangle = 15$ MeV, in the numerical calculation. This approximation further reduces the probabilities to functions of only n and ϕ_{13} . The survival probabilities for ν_e and $\bar{\nu}_e$ can be plotted in the $n - \sin^2 \phi_{13}$ space, as shown in Fig. 2 and Fig. 3, respectively. It is seen that if $n < -6$, the values of all the probability functions approach a constant ~ 0.6 regardless of the mass hierarchy and the value of ϕ_{13} . Thus, the mass hierarchies are indistinguishable and the information about ϕ_{13} is lost if $n < -6$. As n increases from -6 , the probability functions of ν_e in Fig. 2 are seen to drop through a transition near $n \sim -5$, while that of $\bar{\nu}_e$ in Fig. 3 jump through a transition near $n \sim -4.5$. Furthermore, P_{nor} and \bar{P}_{inv} exhibit an extra non-trivial structure for $n > -4$. In the following discussion, we divide n into three regions: $n < -6$, $-6 < n < -4$, and $n > -4$. The probability functions for ν_e and $\bar{\nu}_e$ shall be discussed separately.

A. P_{nor} and P_{inv}

We first note that the condition $P_{nor} = P_{inv}$ is satisfied if the higher crossing is extremely non-adiabatic: $P_h \rightarrow 1$, as implied by Eqs. (1) and (3). Thus, P_{nor} and P_{inv} are indistinguishable if the values of n and $\sin^2 \phi_{13}$ result in $P_h \rightarrow 1$, which occurs in part of the $n - \sin^2 \phi_{13}$ parameter space, as can be seen by comparing Figs. 2(a) and 2(b). To account for the n -dependent transition of both P_{nor} and P_{inv} in the range $-6 < n < -4$, we note that the adiabatic parameter at the lower crossing takes the form

$$\gamma_l \simeq \frac{0.43 \times 10^{-5}}{|n|} (0.39 \times 10^{-30})^{\frac{1}{n}}, \quad (8)$$

which yields $\gamma_l \ll 1$ and $P_l \simeq \cos^2 \theta_{12}$ (non-adiabatic transition) for $n < -6$. On the other hand, the same expression leads to $\gamma_l \gg 1$ and $P_l \approx 0$ (adiabatic transition) when $n > -4$. It is clear that γ_l goes through a transition from $\gamma_l \ll 1$ to $\gamma_l \gg 1$ as n varies from $n \sim -6$ to $n \sim -4$. A simple calculation shows that $P_{inv} \simeq P_{nor} \approx 0.6$ at $n = -6$, while $P_{inv} \simeq P_{nor} \approx 0.3$ at $n = -4$ if $\sin^2 \phi_{13} < 10^{-3}$. This result implies that the uncertainty of n between $n = -4$ and $n = -6$ could lead to a variation of the survival probability by a factor of two and complicate the interpretation of the ν_e events.

The 3D plots of P_{inv} and P_{nor} in the $n - \sin^2 \phi_{13}$ space become distinguishable for $n > -4$ if $P_h \neq 1$. Note that for $n > -4$, $P_l \approx 0$ and P_{nor} becomes

$$P_{nor} \simeq \sin^2 \phi_{13} + P_h (\sin^2 \theta_{12} \cos^2 \phi_{13} - \sin^2 \phi_{13}), \quad (9)$$

where P_h is given by Eq. (5), and the adiabaticity parameter γ_h in P_h is given by Eq. (6):

$$\gamma_h \simeq \frac{10^{-4}}{|n|} (37.6 \times 10^{-30} \times \cos 2\phi)^{\frac{1}{n}} \frac{\sin^2 2\phi_{13}}{\cos 2\phi_{13}}. \quad (10)$$

For $n > -4$, the subtle dependence of P_{nor} on n and $\sin^2 \phi_{13}$ can be seen clearly from Eq. (9) and Fig. 2. For small $|n|$ and large ϕ_{13} (near the right corner of Fig. 2(a)), the higher level crossing is adiabatic ($\gamma_h \gg 1$ and $P_h \approx 0$). Thus, the first term in Eq. (9)

dominates and $P_{nor} \simeq \sin^2 \phi_{13} \ll 1$. On the other hand, the higher level crossing becomes non-adiabatic ($\gamma_h \ll 1$ and $P_h \approx 1$) for relatively larger $|n|$ and smaller ϕ_{13} . Thus, the second term in Eq. (9) begins to dominate, and $P_{nor} \simeq \sin^2 \theta_{12} \approx 0.3$. Note that since the two values of P_h , $P_h \approx 1$ and $P_h \approx 0$, give rise to the above two distinct values of P_{nor} representing the two sides of the fast transition area in Fig. 2(a), the condition $P_h = 1/2$ should reasonably describe the fast transition of P_{nor} for $n > -4$. Furthermore, due to the smallness of the upper bound on ϕ_{13} , the arguments in the numerator of Eq. (5) satisfy the relation

$$\frac{\pi}{2} \gamma_h F_h \ll \frac{\pi}{2} \frac{\gamma_h F_h}{\sin^2 \phi_{13}}, \quad (11)$$

which implies that

$$\exp(-\frac{\pi}{2} \gamma_h F_h) \approx \frac{1}{2} \quad (12)$$

at the narrow transition region. The condition Eq. (12) leads to $G_h \approx 1$, where

$$G_h \equiv \frac{\pi}{4(\ln 2)} \frac{1}{|n|} \left(\frac{\Delta m_{32}^2}{E_\nu} \right) \left(\frac{\frac{\Delta m_{32}^2}{E_\nu} \cos 2\phi_{13}}{c} \right)^{\frac{1}{n}} \left(\frac{\sin^2 2\phi_{13}}{\cos 2\phi_{13}} \right) F_h. \quad (13)$$

Since $F_h \sim 1$ in the region of interest ($n > -4$ and $\sin^2 \phi_{13} < 10^{-2}$), the above condition can be approximated as

$$G_h(n, \phi_{13}) \simeq \frac{2.3 \times 10^{-4}}{|n|} (37.6 \times 10^{-30} \times \cos 2\phi_{13})^{\frac{1}{n}} \frac{\sin^2 2\phi_{13}}{\cos 2\phi_{13}} \approx 1. \quad (14)$$

It can be shown that $P_h \approx 1$ if $G_h(n, \phi_{13}) < 1$ and $P_h \approx 0$ if $G_h(n, \phi_{13}) > 1$. Take $n = -3$ for example, the sudden probability transition is located near $\sin^2 \phi_{13} \sim 10^{-5}$. Thus, $P \sim 0$ if $\sin^2 \phi_{13} > 10^{-5}$, which is unique to the normal mass hierarchy. However, if $\sin^2 \phi_{13} < 10^{-5}$, then $P \sim 0.3$ for both the normal and the inverted mass hierarchies. This feature is clearly seen in Fig. 2.

Eq. (14) suggests that a slight variation of the power may cause an ambiguity in the interpretation of ϕ_{13} and the mass hierarchy that are derived from the observation of neutrino events. Note that although the numerical values in Eq. (14) vary with the input parameters, the physical content remains unaltered. We summarize this subsection as follows.

1. Given the input values of Δm_{21}^2 , $\sin^2 \theta_{12}$, and c , it can be shown that P_l is adiabatic ($\gamma_l \gg 1$) for $n > -4$ and non-adiabatic ($\gamma_l \ll 1$) for $n < -6$.
2. For the normal mass hierarchy, the two distinct values of P due to $P_h \approx 1$ and $P_h \approx 0$ for $n > -4$ are separated by the condition Eq. (14).
3. In principle, a direct observation of the ν_e events could be used to distinguish the mass hierarchy if the values of n and ϕ_{13} result in $P_h \neq 1$, as suggested by Figs. 2(a) and 2(b).

B. \bar{P}_{nor} and \bar{P}_{inv}

The survival probabilities of $\bar{\nu}_e$ are described by Eq. (2) and Eq. (4) for the normal and the inverted mass hierarchies, respectively. The 3D plots of \bar{P}_{nor} and \bar{P}_{inv} are shown in Fig. 3. Note that $P_h = \bar{P}_h$, and that $\bar{\gamma}_l$, \bar{F}_l , and \bar{P}_l can be obtained respectively from γ_l , F_l , and P_l by the swap $\sin \theta_{12} \leftrightarrow \cos \theta_{12}$. Since $\bar{P}_l \simeq \sin^2 \theta_{12} \approx 0.3$ and $\bar{P}_h \approx 1$ for $n < -6$, it follows that

$$\bar{P}_{nor} = \bar{P}_{inv} \simeq \cos^2 \phi_{13} \cos^2 \theta_{12} (1 - \sin^2 \theta_{12}) + \cos^2 \phi_{13} \sin^4 \theta_{12} \approx 0.6. \quad (15)$$

This explains why the mass hierarchies are also indistinguishable from observing the $\bar{\nu}_e$ events if $n < -6$. In addition, the transition behavior of \bar{P}_{nor} and \bar{P}_{inv} for $-6 < n < -4$ can be explained in the way similar to that of P_{nor} and P_{inv} .

For $n > -4$, the lower level crossing becomes adiabatic: $\bar{P}_l \approx 0$. If the higher crossing remains non-adiabatic ($\bar{P}_h \approx 1$), it leads to $\bar{P}_{nor} \simeq \bar{P}_{inv} \simeq \cos^2 \phi_{13} \cos^2 \theta_{12} \approx 0.7$, which is slightly higher than that for $n < -6$. However, when \bar{P}_h departs from unity, there would be a sudden drop of the probability function if the mass hierarchy is inverted: $\bar{P}_{inv} \simeq \sin^2 \phi_{13} \ll 1$, as shown in Fig. 3(b). The sudden drop of this probability function is similar to that of P_{nor} for the neutrino sector, and can be characterized by the same condition for that of the neutrino, Eq. (14), with a slight change of the numerical values. The properties of all the probability functions for $n > -4$ and $n < -6$ are summarized in Table 1.

IV. POWER-LAW DENSITY PROFILE, ϕ_{13} , AND MASS HIERARCHIES

We shall now investigate whether and how the information about the mass hierarchy and ϕ_{13} could be extracted from the observation of supernova neutrinos. Although the uncertainty in the density profile is unavoidable due to incomplete knowledge of the supernova mechanism, the results in Fig. 2 and Fig. 3 may still provide a useful guideline. We summarize the hints as follows.

1. As suggested by Figs. 2(a) and 2(b), the mass hierarchy may be identified as normal if the survival probability of ν_e is observed to be extremely small, *i.e.*, if $P \ll 0.3$. On the other hand, an extremely small survival probability for $\bar{\nu}_e$, $\bar{P} \ll 0.7$, would signal an inverted hierarchy, as suggested by Figs. 3(a) and 3(b). Although this feature provides no information about the mixing angle ϕ_{13} , it predicts the mass hierarchy without knowing the details of the density shape, *i.e.*, the exact value of n is irrelevant. Note that the numerical values would vary slightly with the input parameters.
2. If $P \simeq \bar{P} \approx 0.6$ is observed, the power n of the density profile is limited to $n < -6$ and a significant deviation from $n = -3$ is implied. The information about mass hierarchy or ϕ_{13} is unavailable in this case.
3. If $\bar{P} < P$ can be deduced from experiments, then $n > -4$, $G_h(n, \phi_{13}) > 1$, and the inverted mass hierarchy are implied. These conditions lead to $\sin^2 \phi_{13} > 4 \times 10^{-4}$. On the other hand, if $\bar{P} > P$ is observed, it implies that (i) the mass hierarchy is normal and ϕ_{13} is undetermined (Figs. 2(a) and 3(a)), or (ii) the mass hierarchy is inverted

and $G_h(n, \phi_{13}) < 1$ (Figs. 2(b) and 3(b)). A further observation of the Earth matter effect may be useful in selecting the correct scenario.

4. From Figs. 2(a) and 3(b), it is seen that ϕ_{13} can be sensitive to the direct observation of P_{nor} or \bar{P}_{inv} in only part of the parameter space. As discussed earlier, the prediction of ϕ_{13} depends crucially on the exact value of n in this part of parameter space. Thus, it is very difficult to establish a satisfactory constraint on ϕ_{13} from a direct observation of P or \bar{P} alone. For example, Eq. (14) suggests that a deviation of ± 0.5 from $n = -3$ could result in an uncertainty in the prediction of ϕ_{13} by up to two orders of magnitude. A better knowledge of n or an extended analysis that includes the Earth matter effect would help set the constraint of this tiny mixing angle.

V. OBSERVATION OF EARTH MATTER EFFECTS

The regeneration effect of the supernova neutrinos when crossing the Earth has been widely discussed [12–14, 16, 26, 27]. Since the Earth matter density, $\rho_E \sim$ a few g/cm^3 , is roughly the same order of magnitude as the density for the lower level crossing in a supernova, the neutrino fluxes may receive sizable modification due to the oscillation effects in Earth. In general, the Earth matter effect is signaled by the flux difference observed at two terrestrial detectors $D^{(1)}$ and $D^{(2)}$ [12]:

$$f_e^{(1)} - f_e^{(2)} \simeq P_h(1 - 2P_l)(P_{2e}^{(1)} - P_{2e}^{(2)})(f_e^0 - f_x^0), \quad (16)$$

$$f_{\bar{e}}^{(1)} - f_{\bar{e}}^{(2)} \simeq (1 - 2\bar{P}_l)(P_{1e}^{(1)} - P_{1e}^{(2)})(f_{\bar{e}}^0 - f_{\bar{x}}^0), \quad (17)$$

for the normal mass hierarchy, and

$$f_e^{(1)} - f_e^{(2)} \simeq (1 - 2P_l)(P_{2e}^{(1)} - P_{2e}^{(2)})(f_e^0 - f_x^0), \quad (18)$$

$$f_{\bar{e}}^{(1)} - f_{\bar{e}}^{(2)} \simeq P_h(1 - 2\bar{P}_l)(P_{1e}^{(1)} - P_{1e}^{(2)})(f_{\bar{e}}^0 - f_{\bar{x}}^0), \quad (19)$$

for the inverted mass hierarchy. In the above expressions, $f_e^{(i)}$ ($f_{\bar{e}}^{(i)}$) is the observed ν_e ($\bar{\nu}_e$) flux at the detector $D^{(i)}$, $P_{je}^{(i)}$ ($\bar{P}_{je}^{(i)}$) is the probability that a ν_j ($\bar{\nu}_j$) arriving at the Earth surface is detected as a ν_e ($\bar{\nu}_e$) at the detector, and $f_{e,x}^0$ ($f_{\bar{e},\bar{x}}^0$) is the initial flux for the specific neutrino (antineutrino), with $x = \mu, \tau$.

The Earth matter effects could affect (i) ν_e flux only; (ii) $\bar{\nu}_e$ flux only; (iii) both ν_e and $\bar{\nu}_e$ fluxes. We assume that the suppression of matter effect, if any, is due solely to the smallness of P_h . Possible consequences of the above three scenarios are summarized in Table II and discussed below:

1. If the Earth effect is observed only in the ν_e flux ($f_e^{(1)} - f_e^{(2)} \neq 0$ and $f_{\bar{e}}^{(1)} - f_{\bar{e}}^{(2)} = 0$), it requires an extremely small P_h under the inverted hierarchy, as can be seen from Eqs. (18) and (19). Results in Table I show that $P_h \rightarrow 0$ is possible when $n > -4$ and $G_h(n, \phi_{13}) > 1$. These conditions lead to a lower bound on ϕ_{13} : $\sin^2 \phi_{13} > 4 \times 10^{-4}$.

2. If the Earth effect is observed only in the $\bar{\nu}_e$ flux ($f_e^{(1)} - f_e^{(2)} = 0$ and $f_{\bar{e}}^{(1)} - f_{\bar{e}}^{(2)} \neq 0$), then Eqs. (16) and (17) suggest that P_h is extremely small and the mass hierarchy is normal. This leads to the same constraint: $\sin^2 \phi_{13} > 4 \times 10^{-4}$.
3. If the Earth matter effect is observed in both the ν_e and the $\bar{\nu}_e$ fluxes, then $P_h \neq 0$ is required. It can be seen from Table I that this condition can be satisfied if (i) $n > -4$ and $G_h(n, \phi_{13}) < 1$, or (ii) $n < -6$. Note that, as discussed earlier, the observation of supernova neutrino loses its predictive power if $n < -6$. Even from the first condition: $n > -4$ and $G_h(n, \phi_{13}) < 1$, an evident constraint on ϕ_{13} is still not available unless the uncertainty of n can be reduced significantly. Furthermore, this scenario provides no information about the mass hierarchy.

There is a possibility that the constraint on ϕ_{13} might be available from checking the signs of $f_e^{(1)} - f_e^{(2)}$ and $f_{\bar{e}}^{(1)} - f_{\bar{e}}^{(2)}$, if the Earth matter effect is observed in both the ν_e and the $\bar{\nu}_e$ fluxes. Suppose that one of the two detectors, $D^{(2)}$, is not shielded by the Earth matter. It then leads to the replacements: $P_{2e}^{(2)} \rightarrow |U_{e2}|^2$ and $\bar{P}_{1e}^{(2)} \rightarrow |U_{e1}|^2$, which satisfy $P_{2e}^{(1)} \geq |U_{e2}|^2$ and $\bar{P}_{1e}^{(1)} \geq |U_{e1}|^2$. Since the average energies obey the hierarchy: $\langle E(\nu_e) \rangle < \langle E(\nu_x) \rangle$ and $\langle E(\bar{\nu}_e) \rangle < \langle E(\bar{\nu}_x) \rangle$, there exists an energy E_c (\bar{E}_c) at which $f_e^0 - f_x^0$ ($f_{\bar{e}}^0 - f_{\bar{x}}^0$) changes sign [12]. In general, $f_e^0 - f_x^0 > 0$ ($f_{\bar{e}}^0 - f_{\bar{x}}^0 > 0$) in $E < E_c$ ($E < \bar{E}_c$), and $f_e^0 - f_x^0 < 0$ ($f_{\bar{e}}^0 - f_{\bar{x}}^0 < 0$) in $E > E_c$ ($E > \bar{E}_c$). Furthermore, the magnitude of P_l varies from 0 (for $n > -4$) to $\cos^2 \theta_{12} \approx 0.7$ (for $n < -6$), and \bar{P}_l varies from 0 to $\sin^2 \theta_{12} \approx 0.3$. Thus, $1 - 2\bar{P}_l$ is always positive, while $1 - 2P_l$ flips sign over the transition region $-6 < n < -4$. The above arguments suggest the following:

1. If $f_e^{(1)} - f_e^{(2)}$ and $f_{\bar{e}}^{(1)} - f_{\bar{e}}^{(2)}$ are both observed to be negative at the high energy end of the spectrum, or both positive at the low energy end, then it implies $1 - 2P_l > 0$ (from Table I), $n > -4$, and $G_h(n, \phi_{13}) > 1$. This leads to the constraint: $\sin^2 \phi_{13} > 4 \times 10^{-4}$. However, the mass hierarchy is undetermined from this result.
2. If $f_e^{(1)} - f_e^{(2)}$ and $f_{\bar{e}}^{(1)} - f_{\bar{e}}^{(2)}$ are of opposite signs, then $1 - 2P_l < 0$, and $n < -6$. No further information about ϕ_{13} or the mass hierarchy is available.

We summarize the above results in Table III.

VI. SUMMARY AND CONCLUSION

The supernova neutrinos may provide a promising future for the study of unknown neutrino properties. However, the detailed knowledge of the core-collapse supernova event is still far from complete. In addition to the uncertainties in the original neutrino fluxes and in the effects due to the shock propagation, the original neutrino spectra can be further deformed by the flavor conversion when the neutrinos propagate through matter of uncertain density profiles.

In this work, parameters obtained from recent experiments are taken as the input for the purpose of analyzing the survival probabilities of ν_e and $\bar{\nu}_e$. It is suggested that the influence coming from the energy variation can be excluded. The effort is then focused on investigating how the unknown mass hierarchy, the mixing angle ϕ_{13} , and the uncertainty in n would affect the probability functions.

It is shown that the non-trivial behavior of the probability functions can be well illustrated by the 3D plots in the $n - \sin^2 \phi_{13}$ parameter space, and that the uncertainty of n could lead to ambiguity in the interpretation of ϕ_{13} and the mass hierarchy. Roughly speaking, the probability functions behave differently in three regions of the parameter space: $n < -6$, $-6 < n < -4$, and $n > -4$. As far as the mass hierarchy and the mixing angle ϕ_{13} are concerned, the information is lost if the supernova neutrinos encounter a relatively steep density profile ($n < -6$) near the location of flavor conversion. For a not as steep density profile ($-6 < n < -4$), all the probability functions go through a transition that is governed by the variation of n . This transition depends only very weakly on the mass hierarchy and ϕ_{13} . For $n > -4$, the probability functions vary with the mass hierarchy, the value of n , and ϕ_{13} in a non-trivial fashion, as depicted clearly by Figs. 2 and 3. Furthermore, this non-trivial structure is found to be divided by a function of n and ϕ_{13} through the condition Eq. (14).

For the qualitative observation of the Earth matter effect, it can be shown that the constraint on ϕ_{13} would be available only if $n > -4$. However, the exact value of n is irrelevant to the constraint as long as n is greater than -4 .

It is hoped that Eq. (14) and the 3D plots of the probability functions could provide a guideline to finding useful observables from the future supernova neutrino experiments, and to better help shed light on the desired understanding of the neutrino properties. We shall return to this topic in the near future.

ACKNOWLEDGMENTS

S. -H. C. is supported by the National Science Council of Taiwan under the grant no. 94-2112-M-182-004. T. K. K. is supported in part by the DOE, grant no. DE-FG02-91ER40681.

REFERENCES

- [1] Super-KamioKande Collaboration, Y. Fukuda *et al.*, Phys. Rev. Lett. **82**, 2644 (1999).
- [2] SNO Collaboration, R. Q. Ahmad *et al.*, Phys. Rev. Lett. **87**, 071301 (2001).
- [3] Super-KamioKande Collaboration, M. B. Smy *et al.*, Phys. Rev. D **69**, 011104 (2004).
- [4] KamLAND Collaboration, K. Eguchi *et al.*, Phys. Rev. Lett. **90**, 021802 (2003).
- [5] K2K Collaboration, M. H. Ahn *et al.*, Phys. Rev. Lett. **90**, 041801 (2003).
- [6] CHOOZ Collaboration, M. Apollonio *et al.*, Phys. Lett. B **466**, 415 (1999).
- [7] Palo Verde Collaboration, F. Boehm *et al.*, Phys. Rev. D **62**, 092005 (2000).
- [8] See, *e.g.*, G. G. Raffelt, Nucl. Phys. Proc. Suppl. **110**, 254 (2002).
- [9] L. Wolfenstein, Phys. Rev. D **17**, 2369 (1978).
- [10] S. P. Mikheyev and A. Yu. Smirnov, Sov. J. Nucl. Phys. **42**, 913 (1985).
- [11] Kamiokande Collaboration, K. S. Hirata *et al.*, Phys. Rev. Lett. **58**, 1490 (1987); IMB Collaboration, R. M. Bionta *et al.*, *ibid.* **58**, 1494 (1987); E. N. Alexeyev *et al.*, JETP Lett. **45**, 589 (1987).
- [12] A. S. Dighe and A. Yu. Smirnov, Phys. Rev. D **62**, 033007 (2000).
- [13] G. L. Fogli, E. Lisi, D. Montanino, and A. Palazzo, Phys. Rev. D **65**, 073008 (2002).
- [14] C. Lunardini and A. Yu. Smirnov, JCAP **0306**, 009 (2003).
- [15] A. S. Dighe, M. T. Keil, and G. G. Raffelt, JCAP **0306**, 005 (2003).
- [16] A. Bandyopadhyay *et al.*, arXiv:hep-ph/0312315.
- [17] H. Davoudiasl and P. Huber, arXiv:hep-ph/0504265.
- [18] S. -H. Chiu and T. K. Kuo, Phys. Rev. D **61**, 073015 (2000).
- [19] See, *e.g.*, G. L. Fogli, E. Lisi, and A. Mirizzi, Phys. Rev. D **68**, 033005 (2003); R. C. Schirato and George M. Fuller, arXiv:astro-ph/0205390; K. Takahashi, K. Sato, H. E. Dalhed, and J. R. Wilson, Astropart. Phys. **20**, 189-193 (2003), and the references therein.
- [20] T. K. Kuo and J. Pantaleone, Phys. Rev. D **39**, 1930 (1989).
- [21] L. Landau, Phys. Z. Sowjetunion **2**, 46 (1932); C. Zener, Proc. R. Soc. London **A137**, 696 (1932).
- [22] T. K. Kuo and J. Pantaleone, Rev. Mod. Phys. **61**, 937 (1989).
- [23] T. K. Kuo and J. Pantaleone, Phys. Rev. D **37**, 298 (1988).
- [24] A. Friedland, Phys. Rev. D **64**, 013008 (2001).
- [25] M. Kachelrieß, A. Strumia, R. Tomàs, and J. W. F. Valle, Phys. Rev. D **65**, 073016 (2002).
- [26] A. N. Ioannisian, N. A. Kazarian, A. Yu. Smirnov, and D. Wyler, Phys. Rev. D **71**, 033006 (2005).
- [27] E. Kh. Akhmedov, C. Lunardini, A. Yu. Smirnov, Nucl. Phys. B **643**, 339 (2002).

TABLES

	$n > -4$	$n < -6$
$P_h(\bar{P}_h)$	0, if $G_h(n, \phi_{13}) > 1$ 1, if $G_h(n, \phi_{13}) < 1$	$\cos^2 \phi_{13} \approx 1$
P_l	0	$\cos^2 \theta_{12} \approx 0.7$
\bar{P}_l	0	$\sin^2 \theta_{12} \approx 0.3$
P	normal: $\sin^2 \theta_{12} P_h + \sin^2 \phi_{13} (1 - P_h)$ $\simeq \sin^2 \phi_{13} \approx 0$, if $G_h(n, \phi_{13}) > 1$ $\simeq \sin^2 \theta_{12} \approx 0.3$, if $G_h(n, \phi_{13}) < 1$ inverted: $\sin^2 \theta_{12} \approx 0.3$	$\sin^2 \theta_{12} + (\cos^2 \theta_{12} - \sin^2 \theta_{12}) \cos^2 \theta_{12} \approx 0.6$
\bar{P}	normal: $\cos^2 \phi_{13} \cos^2 \theta_{12} \approx 0.7$ inverted: $\cos^2 \theta_{12} P_h + \sin^2 \phi_{13} (1 - P_h)$ $\simeq \sin^2 \phi_{13} \approx 0$, if $G_h(n, \phi_{13}) > 1$ $\simeq \cos^2 \theta_{12} \approx 0.7$, if $G_h(n, \phi_{13}) < 1$	$\cos^2 \theta_{12} + (\sin^2 \theta_{12} - \cos^2 \theta_{12}) \sin^2 \theta_{12} \approx 0.6$

TABLE I. Properties of the probability functions for $n > -4$ and $n < -6$.

matter effect	requirement	prediction
ν_e only	$P_h \rightarrow 0, n > -4, G_h(n, \phi_{13}) > 1$	inverted, $\sin^2 \phi_{13} > 4 \times 10^{-4}$
$\bar{\nu}_e$ only	$P_h \rightarrow 0, n > -4, G_h(n, \phi_{13}) > 1$	normal, $\sin^2 \phi_{13} > 4 \times 10^{-4}$
both ν_e and $\bar{\nu}_e$	$P_h \neq 0$	*

TABLE II. Predicting the mass hierarchy and ϕ_{13} from possible scenarios of the Earth matter effects. (* See Table III for further predictions.)

	\bar{f}	f	requirement	prediction
$E > E_c, (E > \bar{E}_c)$	-	+	$f_e^0 - f_x^0 < 0, 1 - 2P_l < 0$	$n < -6$
(high energy end)	-	-	$f_e^0 - f_x^0 < 0, 1 - 2P_l > 0$	$n > -4, \sin^2 \phi_{13} > 4 \times 10^{-4}$
$E < E_c, (E < \bar{E}_c)$	+	+	$f_e^0 - f_x^0 > 0, 1 - 2P_l > 0$	$n > -4, \sin^2 \phi_{13} > 4 \times 10^{-4}$
(low energy end)	-	-	$f_e^0 - f_x^0 > 0, 1 - 2P_l < 0$	$n < -6$

TABLE III. Predicting ϕ_{13} and n from the signs of $\bar{f} \equiv f_{\bar{e}}^{(1)} - f_{\bar{e}}^{(2)}$ and $f \equiv f_e^{(1)} - f_e^{(2)}$ if the Earth matter effect is observed in both ν_e and $\bar{\nu}_e$ fluxes. Note that the information about the mass hierarchy is unavailable.

FIGURES

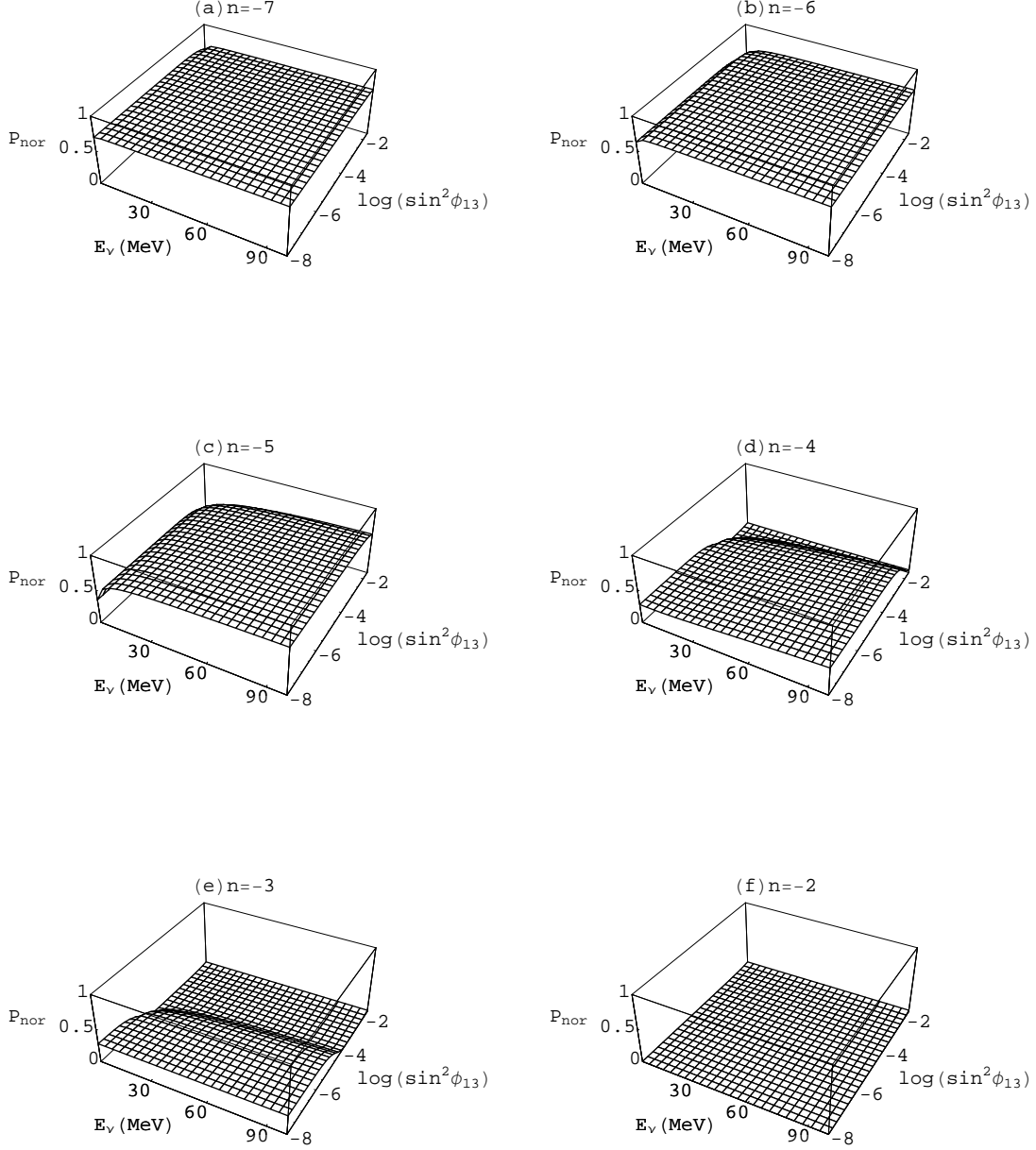


FIG. 1. The 3D plots of $P_{nor} = P_{nor}(E_\nu, \phi_{13})$ for different values of n . The following values are adopted: $\Delta m_{32}^2 = 3.0 \times 10^{-3} \text{eV}^2$, $\Delta m_{21}^2 = 7.0 \times 10^{-5} \text{eV}^2$, $\sin^2 \theta_{12} = 0.8$, and $c = 7.0 \times 10^{31} \text{ g} \cdot \text{cm}^{n-3}$.

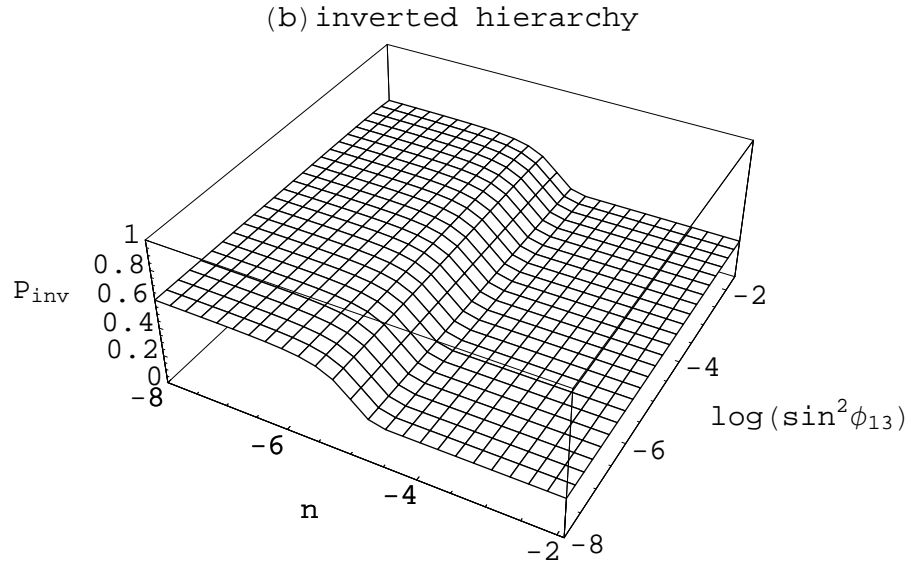
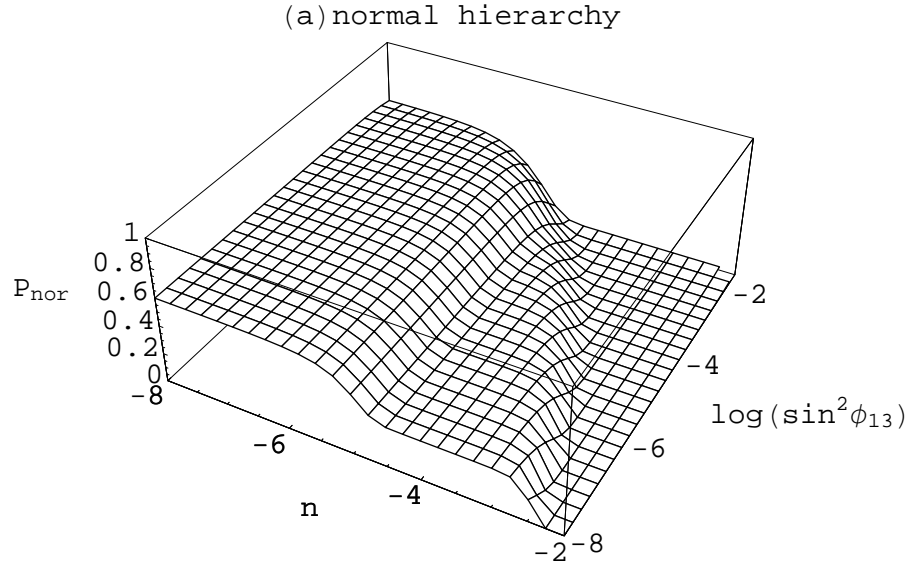


FIG. 2. The 3D plots of $P = P(n, \phi_{13})$ under both (a) the normal, and (b) the inverted mass hierarchies. The average energy $\langle E_\nu \rangle = 12$ MeV is adopted.

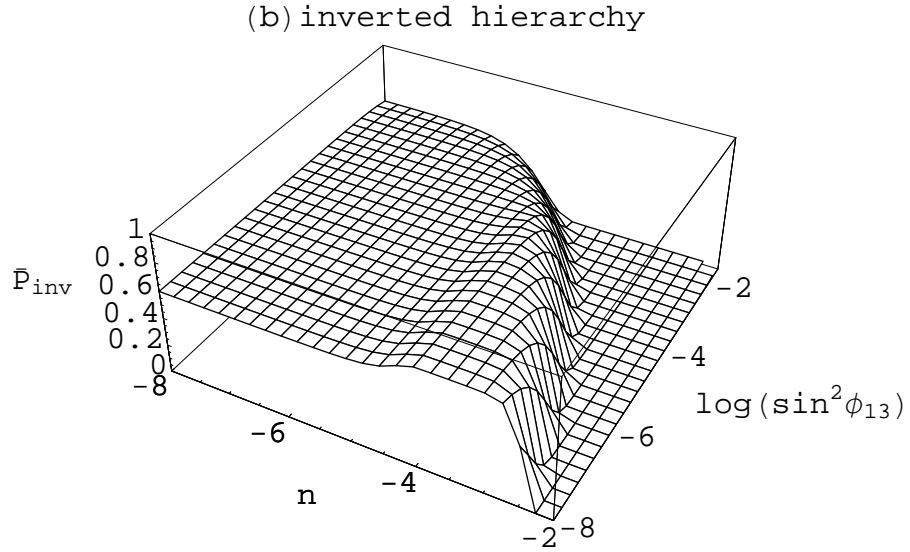
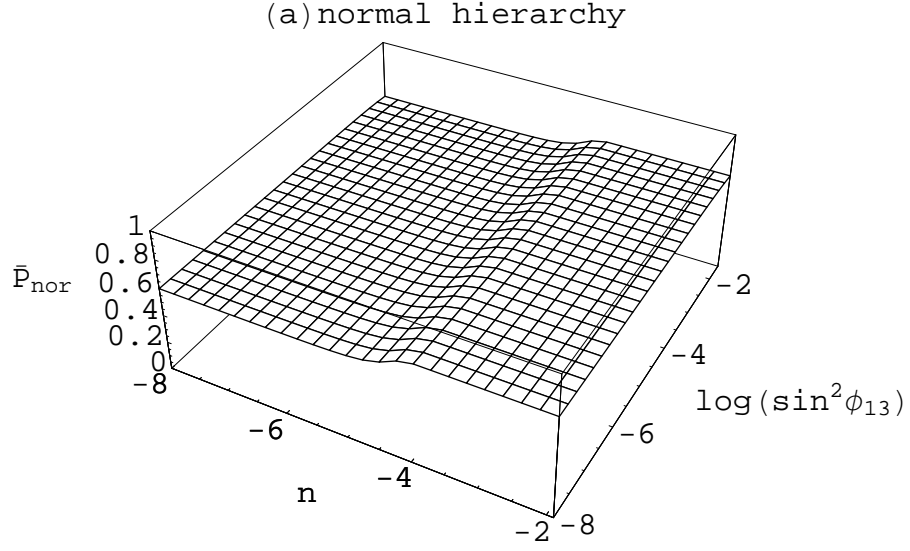


FIG. 3. The 3D plots of $\bar{P} = \bar{P}(n, \phi_{13})$ under both (a) the normal and (b) the inverted mass hierarchies. The average energy $\langle E_{\bar{\nu}} \rangle = 15$ MeV is adopted.